Biophysical Chemistry 196 (2015) 25–32

Contents lists available at ScienceDirect

Biophysical Chemistry

journal homepage: http://www.elsevier.com/locate/biophyschem

Effects of the protein denaturant guanidinium chloride on aqueous hydrophobic contact-pair interactions

Ryan D. Macdonald, Mazdak Khajehpour *

Department of Chemistry, University of Manitoba, Winnipeg, MB R3T 2N2, Canada

HIGHLIGHTS

- We determine how guanidinium chloride affects hydrophobic contact-pair formation.
- Guanidinium chloride disrupts interactions between large hydrophobic pairs.
- Guanidinium chloride does not strongly affect small hydrophobic pairs.

GRAPHICAL ABSTRACT

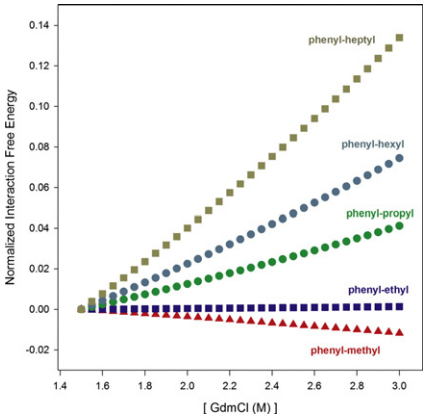

ARTICLE INFO

Article history:
Received 25 July 2014
Received in revised form 20 August 2014
Accepted 20 August 2014
Available online 11 September 2014

Keywords:
Hydrophobic interaction
Fluorescence
Denaturation
Guanidinium chloride

ABSTRACT

Guanidinium chloride (GdmCl) is one of the most common protein denaturants. Although GdmCl is well known in the field of protein folding, the mechanism by which it denatures proteins is not well understood. In fact, there are few studies looking at its effects on hydrophobic interactions. In this work the effect of GdmCl on hydrophobic interactions has been studied by observing how the denaturant influences model systems of phenyl and alkyl hydrophobic contact pairs. Contact pair formation is monitored through the use of fluorescence spectroscopy, i.e., measuring the intrinsic phenol fluorescence being quenched by carboxylate ions. Hydrophobic interactions are isolated from other interactions through a previously developed methodology. The results show that GdmCl does not significantly affect hydrophobic interactions between small moieties such as methyl groups and phenol; while on the other hand, the interaction of larger hydrophobes such as hexyl and heptyl groups with phenol is significantly destabilized.

1. Introduction

Guanidinium chloride (GdmCl) and urea are the two most widely used denaturants in biochemistry. Surprisingly, the mechanism by which they denature proteins is still not completely understood [1–14]. There are two methods by which GdmCl denaturation is thought to occur: indirectly through alteration of the local water hydrogen bonding network and directly through direct interaction (hydrogen bonds and stacking interactions) between the protein and the denaturant. GdmCl is the main focus in this research as there have been few experimental data that focus on the effect of GdmCl on hydrophobic interactions between hydrophobes.

* Corresponding author. Tel.: +1 204 272 1546.
E-mail address: khajehpo@cc.umanitoba.ca (M. Khajehpour).

http://dx.doi.org/10.1016/j.bpc.2014.08.006
0301-4622/

Perhaps one of the simplest hydrophobic interactions is that between two hydrophobes. This simple system lends itself well to investigations of co-solute effects on hydrophobicity [15–19] and there have been quite a few theoretical studies done with regard to studying denaturant effects on pairwise hydrophobic interactions [4,8,20–22]. O'Brien et al. looked at the influence of GdmCl on methane (Me) pairs as well as M^+–M^- ion pairs, where M^+ and M^- are the methane molecules covered in positive and negative charges, respectively, using MD simulations [22]. They found that Me–Me pairs are stabilized by the addition of GdmCl to the aqueous solution, while the M^+–M^- ion pairs were greatly destabilized. Based on these results O'Brien et al. suggest that the guanidinium ion has strong electrostatic interactions with the ion pair, which leads to their destabilization [22].

The hypothesis that electrostatic interactions contribute to the denaturation properties of GdmCl has also been suggested by Godawat et al. Their calculations confirm that small hydrophobic pairs are stabilized by the addition of GdmCl to the aqueous solution; interestingly, the same work also shows that large hydrophobic pairs are destabilized by adding the denaturant [20]. These results were attributed by Godawat et al. to be the result of: (a) the guanidinium ion is "multisite" which promotes van der Waals interactions with large hydrophobes, (b) guanidinium ions are much more concentrated at surfaces of large hydrophobes than in the bulk solution [20,22], and (c) the guanidinium ion's planar shape promotes stacking interactions with protein side chains [23]. Thus, factors other than hydrogen bonding to the polypeptide backbone may contribute significantly to protein denaturation. In fact, hydrogen–deuterium exchange (1D NMR) experiments [24] and neutron diffraction studies [25] indicate that mechanisms other than direct hydrogen bonding to the polypeptide backbone [22,26,27] are involved in guanidinium ion denaturation.

Since interactions other than direct hydrogen bonding play a role in the guanidinium denaturation process, we need to understand how this ion affects hydrophobic interactions. However, most analyses of GdmCl effects are from MD simulations. Therefore, it is vital to also obtain experimental evidence of how this denaturant influences hydrophobicity. This work looks into how GdmCl affects interactions between hydrophobic phenyl and alkyl groups in aqueous solution by examining the quenching of phenol fluorescence by a variety of aliphatic carboxylate ions. Previously, we have developed a methodology for isolating the contribution of phenol–carboxylate interactions to fluorescence quenching data [15,17,19]. Using the same methodology the hydrophobic interactions between phenol and carboxylate ions, in the presence of GdmCl, are quantified. Our results show that the addition of GdmCl has a small effect on aqueous solutions containing small hydrophobic pairs (acetate-phenyl and propionate-phenyl); while adding the denaturant to aqueous solutions of phenyl and large hydrophobes such as butyrate, heptanoate, and octanoate, causes the hydrophobic pairs to destabilize.

2. Experimental

2.1. Materials

Sodium formate, sodium propionate, and taurine were purchased from Sigma-Aldrich (St. Louis, MO). Sodium Acetate, hydrochloric acid solution, and sodium hydroxide were purchased from Fisher Scientific (Hampton, NH). Sodium heptanoate and sodium octanoate were purchased from TCI America (Portland, OR). The phenol was purchased from J.T. Baker Chemical Co. (Phillipsburg, NJ) and guanidinium chloride was purchased from Chem-Impex International Inc. (Wood Dale, IL).

2.2. Methods

Phenol fluorescence was measured in the presence of five quencher (carboxylate ion) concentrations, at each of five different GdmCl concentrations (1.50, 1.88, 2.25, 2.63, and 3.00 M). The addition of quencher would therefore contribute less than 20% to the ionic strength. All samples had 10 mM taurine buffer and 200 μM phenol present. All samples were adjusted to pH 8.5 with concentrated HCl/NaOH. All samples were prepared in triplicate. Steady-state fluorescence spectra were collected using a Fluorolog-3 Horiba Jobin Yvon spectrofluorometer (Edison, NJ). Fluorescence spectra were collected using an excitation wavelength set to 270 nm; excitation and emission slits were set to 5 nm band pass resolution. All samples were measured at room temperature (20 °C) and held in a 10 × 3 mm^2 quartz cuvette. The molar extinction coefficient of phenol in water is 1373 M^{-1} cm^{-1} [28], therefore, no appreciable inner-filter effect corrections need to be applied to the measured phenol fluorescence values. The quenching assays were monitored by changes in fluorescence intensity at the emission maximum of 297 nm as a function of quencher concentration. All data was analyzed by the use of Sigma Plot 12 software (Point Richmond, CA).

3. Results and discussion

3.1. Results

This work uses fluorescence quenching methods to study the effects of GdmCl on hydrophobic pair interactions. Our model system is the contact pairs formed between carboxylate ions and phenol. Phenol fluorescence is known to be quenched by carboxylate ions through dynamic quenching [15–19]. As an example, Fig. 1 shows the effects of sodium acetate on phenol fluorescence, the observed quenching shows a linear Stern–Volmer profile: [29]

$$\frac{F_0}{F} = 1 + K_{SV}[Q] = 1 + k_q\tau[Q]. \quad (1)$$

In this equation, F_0 is the fluorescence of phenol in the absence of quencher, F is the fluorescence of phenol in the presence of Q molar of quencher; the parameter K_{SV} is the Stern–Volmer constant, which is composed of two components: k_q is the quenching rate constant and τ is the fluorescence lifetime of phenol in the absence of a quencher.

In these experiments we have specifically looked at phenol fluorescence being quenched by formate, acetate, propionate, butyrate, heptanoate, and octanoate ions. We have also looked at the effects of GdmCl on the quenching properties of these anions. The addition of GdmCl to phenol in the presence of these quenchers showed no deviation in the linear Stern–Volmer behavior. However, the addition of GdmCl causes a drop in K_{SV} values, which is visualized in Fig. 2. It can also be seen in Fig. 2 that there are outliers in the data points. This may be a result of GdmCl affecting the phenol fluorescence lifetime. We therefore measured the effects of GdmCl on phenol fluorescence in the range of denaturant concentrations studied and observe that GdmCl can slightly increase (approximately 5%) phenol fluorescence. Therefore, we have corrected these small effects on the K_{SV} constants by multiplying the obtained Stern–Volmer parameters by a factor of $I_0/I(C)$:[17]

$$K'_{SV}(C) = K_{SV} \times \frac{I_0}{I(C)} \quad (2)$$

where $K'_{SV}(C)$ is the "corrected" Stern–Volmer constant, I_0 is the fluorescence intensity of phenol at 1.5 M GdmCl, and I(C) is the fluorescence intensity of the same amount of phenol measured at a given guanidinium concentration of C when there is no quencher present. Fig. 3 demonstrates that the correction applied in Eq. (2) makes the fits more linear and demonstrates that the observed outliers in Fig. 2 result from fluorescence lifetime variations. A compilation of measured K_{SV} and corrected $K'_{SV}(C)$ values can be found in Table 1. The $K'_{SV}(C)$ constants show a decline with [GdmCl] and are linearly related to the denaturant's concentration using the

following equation:

$$K'_{SV}(C) = y_0 + \alpha \times [\text{GdmCl}]. \quad (3)$$

The fitting parameters of these plots (Fig. 3) can be found in Table 2. It may be noted that the K_{SV} values of octanoate show larger uncertainties (3 percent relative error) compared to other measurements. This reflects the fact that octanoate solutions at high concentrations exhibit surfactant-like qualities that limit pipetting reproducibility.

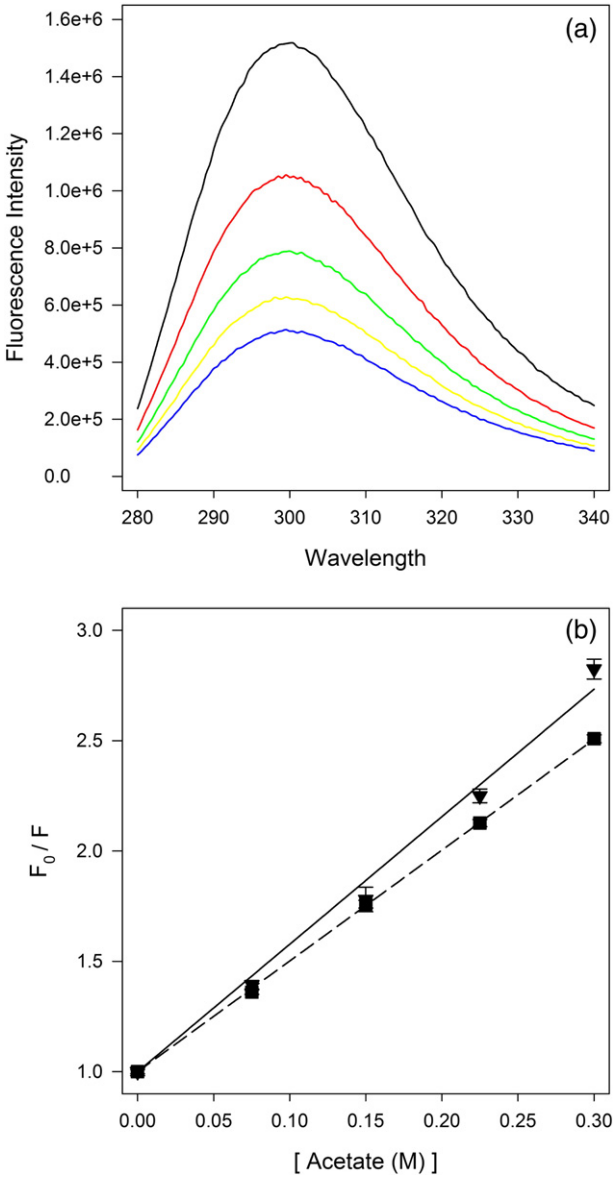

Fig. 1. (a) The quenching of phenol fluorescence by acetate ions (from top to bottom: 0 M, 0.075 M, 0.150 M, 0.225 M, 0.300 M). Excitation and emission slits are set to 2 nm bandpass; (b) Stern–Volmer plots for the quenching of phenol fluorescence by acetate in water (closed triangles) and 3.000 M GdmCl (closed squares).

3.2. Identifying the contribution of contact pair formation to the quenching data

The carboxylate quenching of phenol fluorescence can be represented by Scheme 1:

$$F^* + Q \underset{k_{off}}{\overset{k_{on}}{\rightleftarrows}} [F^* \cdot Q] \xrightarrow{k_{pt}} F + Q$$

where F* is the excited fluorophor, Q is the quencher, [F* · Q] is the encounter complex formed between the quencher and the fluorophor, k_{pt} is the rate of energy transfer between the quencher and the excited fluorophor within the encounter complex, and F is the fluorophor in the ground state. Acetate and formate quench phenol fluorescence by a "reaction controlled" proton transfer process from the excited phenol hydroxide to the acetate/formate ion [16,18]. As previously mentioned, the quenching occurring is dynamic and not static; therefore the Stern–Volmer quenching constant based on the parameters of Scheme 1 can be represented as:

$$K_{SV} = k_q\tau = K_{ec} \times k_{pt} \times \tau \quad (4)$$

where k_q is the rate constant associated with dynamic quenching, τ is the fluorescence lifetime of phenol in the absence of quencher, K_{ec} is the equilibrium constant associated with the formation of the encounter complex, and k_{pt} is the intrinsic rate of proton transfer from the excited phenol to the carboxylate ion. It has been shown that proton transfer occurs significantly when the acceptor and donor moieties are separated by 0–5 water molecules [30]. Therefore, in order for the quenching process to compete with fluorescence the hydroxyl and carboxylate groups must be within 9 Å of one another. Since this value is smaller than the sum of the van der Waals diameters of the fluorophor and quencher molecules, we can assume that there is a high probability that the encounter complex involves reacting molecules coming into van der Waals contact with one another.

3.3. Isolating the contribution of the hydrophobic effect to contact pair formation

We have previously developed a methodology to isolate the hydrophobic contribution to K_{SV} [15,17,19]. The free energy of contact-pair formation between any alkyl-carboxylate and phenol, ΔG_{ec}, is assumed to be comprised of the following two interactions: (a) the interaction between the carboxylate head group and the phenol moiety, and (b) the mostly hydrophobic interaction that exists between phenol and the alkyl tail. This can be represented by:

$$\Delta G_{ec} \approx \Delta G_{head} + \Delta G_{alkyl}. \quad (5)$$

If the formate-phenol contact pair formation energy is subtracted from that of any other phenol-carboxylate, we obtain:

$$\psi = \{\Delta G_{ec}\}_{carboxylate} - \{\Delta G_{ec}\}_{formate} \approx \Delta G_{head} + \Delta G_{alkyl} - \Delta G_{formate}. \quad (6)$$

Any co-solute's effect on contact pair formation can be calculated by subtracting the value of ψ at any given GdmCl concentration S, from that of ψ determined when there is 1.5 M of GdmCl co-solute

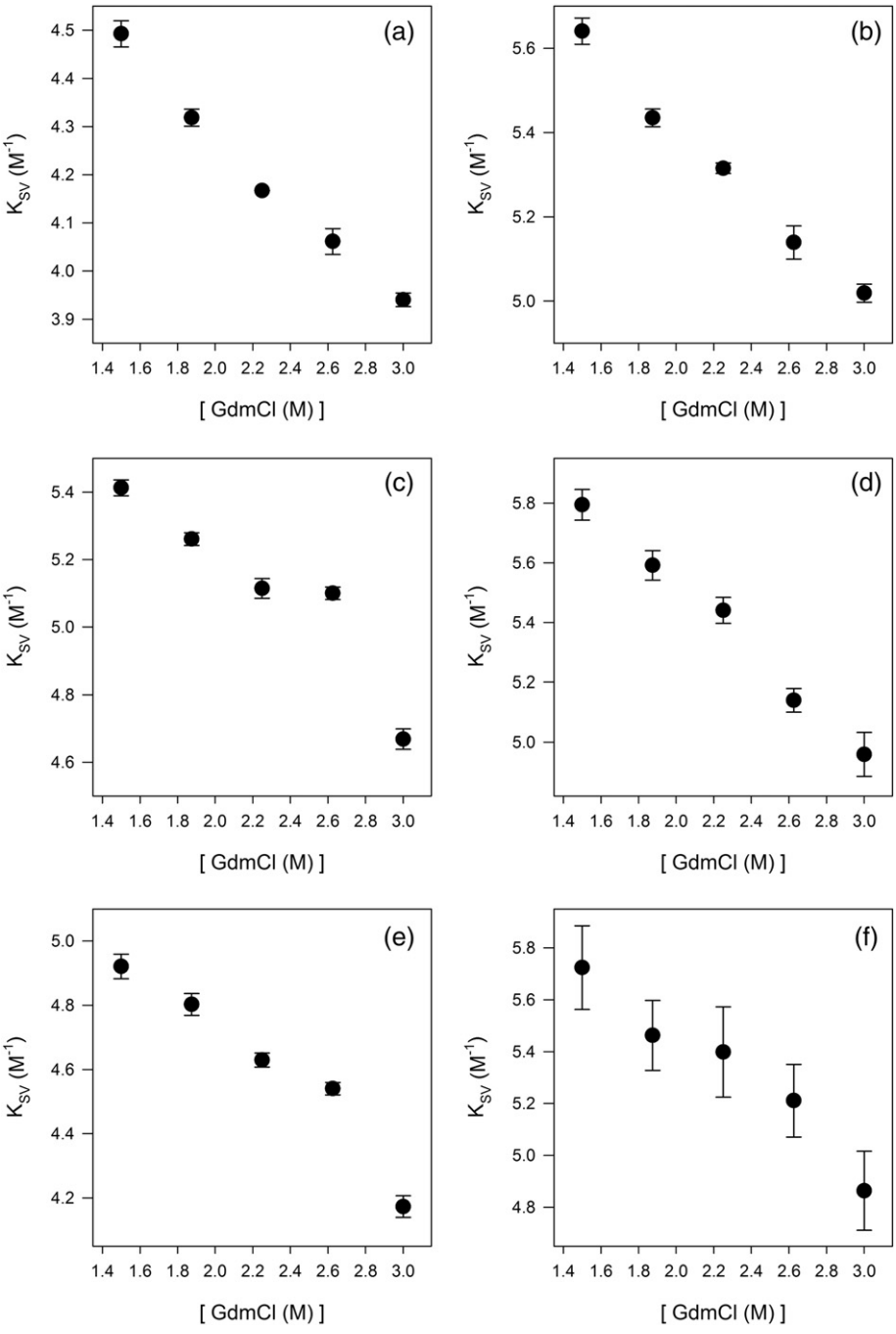

Fig. 2. The effects of GdmCl on the measured Stern–Volmer constant K_{SV} of phenol fluorescence, quenched by: (a) formate, (b) acetate, (c) propionate, (d) butyrate, (e) heptanoate, and (f) octanoate.

present:

$$\Delta\psi = \psi_{[S]} - \psi_{[S]=1.5M} = \left(\Delta G_{head} + \Delta G_{alkyl} - \Delta G_{formate}\right)_{[S]} - \left(\Delta G_{head} + \Delta G_{alkyl} - \Delta G_{formate}\right)_{[S]=1.5M}. \quad (7)$$

The concentration of 1.5 M GdmCl was chosen as our reference point because at lower guanidinium concentrations the quencher species would also contribute significantly to the ionic strength. Rearranging the terms gives the following:

$$\Delta\psi = \left\{(\Delta G_{head})_{[S]} - (\Delta G_{head})_{[S]=1.5M}\right\} - \left\{(\Delta G_{formate})_{[S]} - (\Delta G_{formate})_{[S]=1.5M}\right\} + \left\{\left(\Delta G_{alkyl}\right)_{[S]} - \left(\Delta G_{alkyl}\right)_{[S]=1.5M}\right\}. \quad (7a)$$

If the effects of GdmCl on ΔG_{head} and $\Delta G_{formate}$ are assumed to be linear, which is valid at values close to 1.5 M:

$$(\Delta G_{head})_{[S]} = (\Delta G_{head})_{[S]=1.5M} + m^*[S] \quad (8a)$$

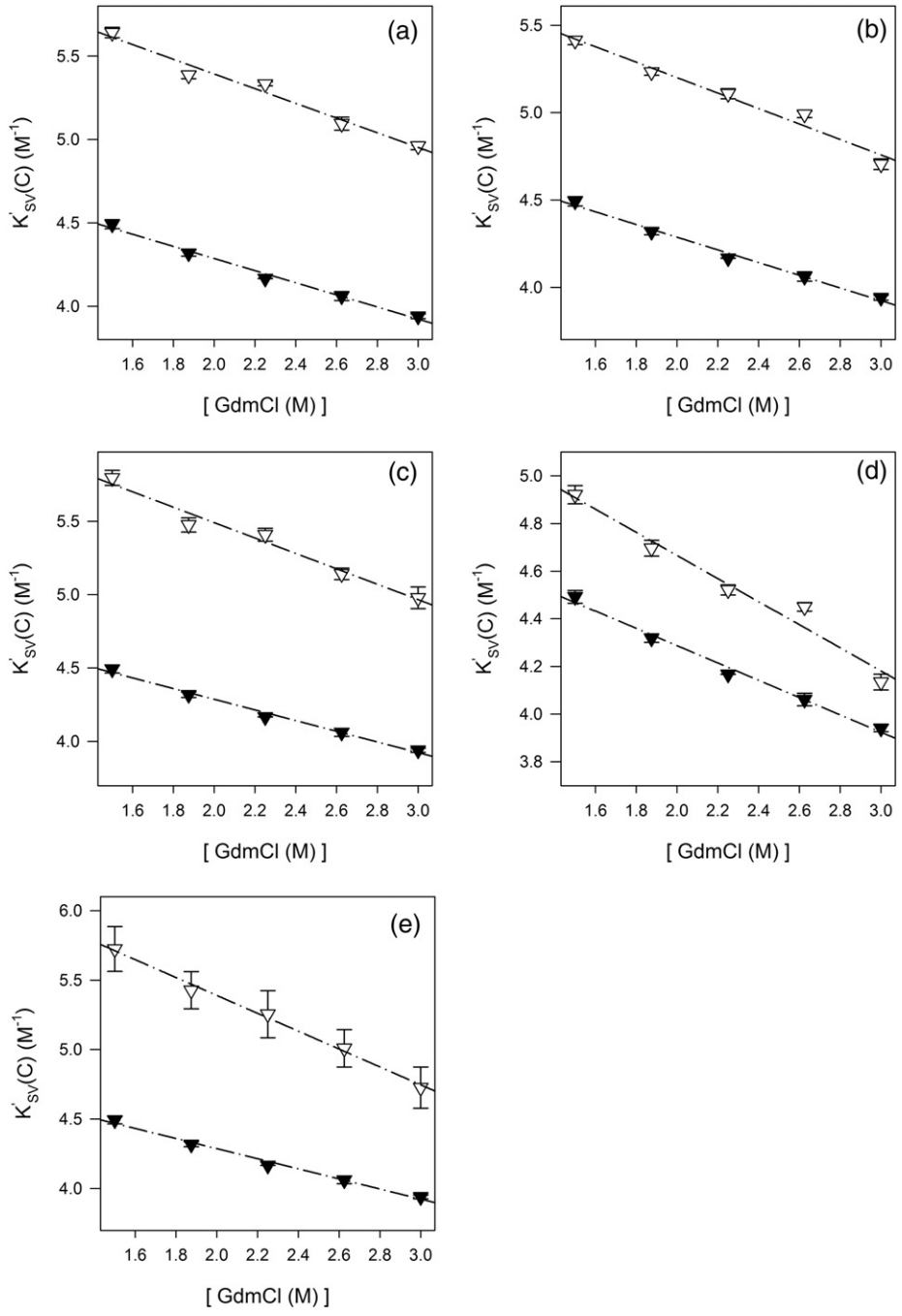

Fig. 3. The effects of GdmCl on the corrected Stern–Volmer constant $K'_{SV}(C)$ of phenol fluorescence, quenched by: (a) formate (closed triangles) and acetate (open triangles), (b) formate (closed triangles) and propionate (open triangles), (c) formate (closed triangles) and butyrate (open triangles), (d) formate (closed triangles) and heptanoate (open triangles), and (e) formate (closed triangles) and octanoate (open triangles).

$$(\Delta G_{\text{formate}})_{[S]} = (\Delta G_{\text{formate}})_{[S]=1.5M} + n^*[S] \tag{8b}$$

where m and n are constants, inserting Eqs. (8a) and (8b) in Eq. (7) results in:

$$\Delta\psi = (m-n)^*[S] + \left\{\left(\Delta G_{\text{alkyl}}\right)_{[S]} - \left(\Delta G_{\text{alkyl}}\right)_{[S]=1.5M}\right\}. \tag{9}$$

Formate is a carboxylate with a pK_a of 3.8, the pK_a of acetic acid is 4.75 (acetic acid) and that of the rest vary between 4.87 and 4.89 [31]. Since the experiments were performed at pH 8.5 all carboxylate groups used are essentially deprotonated. Therefore, electrostatic interactions between phenol and the various alkyl-carboxylate head groups should be similarly affected by GdmCl, which means that the factor of $(m - n)$ is small and similar for all quenchers. Thus, $\Delta\psi$ mostly reflects the difference between the alkyl–phenyl interaction in the presence and absence of additional GdmCl. If the parameter φ is defined for any given alkyl–carboxylate quencher:

$$\Phi = -RT \ln\left(\frac{(K_{SV})_{\text{alkyl-carboxylate}}}{(K_{SV})_{\text{formate}}}\right). \tag{10}$$

Table 1
Compiled measured (K_{sv}) and corrected ($K'_{SV}(C)$) Stern–Volmer constant values of various carboxylate ions, obtained from the quenching of phenol fluorescence. These values are plotted in both Fig. 2 and Fig. 3.

Quencher	[GdmCl] (M)	Measured K_{SV} (M^{-1})	Corrected $K'_{SV}(C)$ (M^{-1})
Formate	1.500	4.49 ± 0.03	4.49 ± 0.03
	1.875	4.34 ± 0.02	4.32 ± 0.02
	2.250	4.10 ± 0.00	4.17 ± 0.00
	2.625	4.09 ± 0.03	4.06 ± 0.03
	3.000	3.92 ± 0.01	3.94 ± 0.01
Acetate	1.500	5.64 ± 0.03	5.64 ± 0.03
	1.875	5.43 ± 0.02	5.39 ± 0.02
	2.250	5.32 ± 0.01	5.33 ± 0.01
	2.625	5.14 ± 0.04	5.09 ± 0.04
	3.000	5.02 ± 0.02	4.96 ± 0.02
Propionate	1.500	5.41 ± 0.02	5.41 ± 0.02
	1.875	5.26 ± 0.02	5.23 ± 0.02
	2.250	5.11 ± 0.03	5.11 ± 0.03
	2.625	5.10 ± 0.02	4.99 ± 0.02
	3.000	4.67 ± 0.03	4.70 ± 0.03
Butyrate	1.500	5.79 ± 0.05	5.79 ± 0.05
	1.875	5.59 ± 0.05	5.47 ± 0.05
	2.250	5.44 ± 0.04	5.41 ± 0.04
	2.625	5.14 ± 0.04	5.14 ± 0.04
	3.000	4.96 ± 0.07	4.98 ± 0.07
Heptanoate	1.500	4.92 ± 0.04	4.92 ± 0.04
	1.875	4.80 ± 0.03	4.70 ± 0.03
	2.250	4.63 ± 0.02	4.52 ± 0.02
	2.625	4.54 ± 0.02	4.45 ± 0.02
	3.000	4.17 ± 0.03	4.13 ± 0.03
Octanoate	1.500	5.72 ± 0.16	5.72 ± 0.16
	1.875	5.46 ± 0.13	5.43 ± 0.13
	2.250	5.40 ± 0.17	5.25 ± 0.17
	2.625	5.21 ± 0.14	5.01 ± 0.13
	3.000	4.86 ± 0.15	4.73 ± 0.15

The values of $K'_{SV}(C)$ are obtained from the linear fits of Table 2. We may now define Δφ:

$$\Delta\Phi = \Phi_{[S]} - \Phi_{[S]=1.5M} = -RT\ln\left(\frac{(K_{SV})_{\text{alkyl-carboxylate}}}{(K_{SV})_{\text{formate}}}\right)_{[S]} + RT\ln\left(\frac{(K_{SV})_{\text{alkyl-carboxylate}}}{(K_{SV})_{\text{formate}}}\right)_{[S]=1.5M}. \quad (11)$$

Substituting Eq. (4) in Eq. (11) we obtain:

$$\Delta\Phi = \Delta\psi - RT\ln\left(\frac{\left(k_{pt}\right)_{\text{alkyl-carboxylate}}}{\left(k_{pt}\right)_{\text{formate}}}\right)_{[S]} + RT\ln\left(\frac{\left(k_{pt}\right)_{\text{alkyl-carboxylate}}}{\left(k_{pt}\right)_{\text{formate}}}\right)_{[S]=1.5M}. \quad (11a)$$

Changes in activation free energies of proton transfer processes due to salt addition are described by linear free energy relationships [16,18].

Table 2
Linear regression fitting parameters obtained from correlating the data in Fig. 3 to Eq. (3).

Quencher	α (M^{-2})	y_0 (M^{-1})	r^2
Formate	−0.36 ± 0.02	5.01 ± 0.05	0.99
Acetate	−0.44 ± 0.04	6.27 ± 0.10	0.97
Propionate	−0.44 ± 0.04	6.08 ± 0.10	0.97
Butyrate	−0.52 ± 0.05	6.54 ± 0.12	0.97
Heptanoate	−0.49 ± 0.05	5.64 ± 0.12	0.97
Octanoate	−0.64 ± 0.03	6.68 ± 0.07	0.99

$$F^* + Q \underset{k_{off}}{\overset{k_{on}}{\rightleftharpoons}} [F^* \bullet Q] \xrightarrow{k_{pt}} F + Q$$

Scheme 1. Suggested mechanism for the quenching of excited state phenol (F^*) fluorescence by quencher molecules Q.

Therefore, the GdmCl dependence of the activation energy can be assumed to be:

$$\Delta\Phi = \Delta\psi + \left(\Delta G^{\ddagger} + \alpha[S]\right)_{\text{alkyl-carboxylate}} - \left(\Delta G^{\ddagger} + \beta[S]\right)_{\text{formate}} - \left(\Delta G^{\ddagger}\right)_{\text{alkyl-carboxylate}} + \left(\Delta G^{\ddagger}\right)_{\text{formate}} = \Delta\psi + (\alpha - \beta)[S]. \quad (12)$$

Phenol is a neutral molecule, therefore there are no primary salt effects on the rate constants and changes in ionic strength will thus have small effects on the activation free energy [32]. In addition to this, the pKa values of the carboxylates are close to each other. Therefore, the factor $(\alpha - \beta)$ should also be small and similar for all alkyl-carboxylate quenchers. Re-writing Eq. (12) gives:

$$\Delta\Phi = \left\{\left(\Delta G_{\text{alkyl}}\right)_{[S]} - \left(\Delta G_{\text{alkyl}}\right)_{[S]=1.5M}\right\} + (m - n + \alpha - \beta)[S] \quad (12a)$$

where the first term isolates the contribution that the interaction between hydrophobic phenyl and alkyl moieties makes to $K'_{SV}(C)$ values; while $(m - n + \alpha - \beta)$ is small and should be essentially constant for the longer carboxylates which have essentially the same pK_a values. The derivative $\frac{d(\Delta\Phi)}{d[\text{GdmCl}]}$ will quantify how the interactions between the hydrophobic phenyl and alkyl moieties are influenced by the addition of GdmCl. Fig. 4 plots Δφ as a function of GdmCl concentration. The values of Δφ are obtained from the corrected Stern–Volmer constants using Eq. (11) and at each given GdmCl concentration the value of $K'_{SV}(C)$ is obtained from Table 2 linear parameters. It can be seen from the Δφ plots that the GdmCl affects phenyl–alkyl contact pairs in a size-dependent fashion. This becomes clear in Fig. 5 when

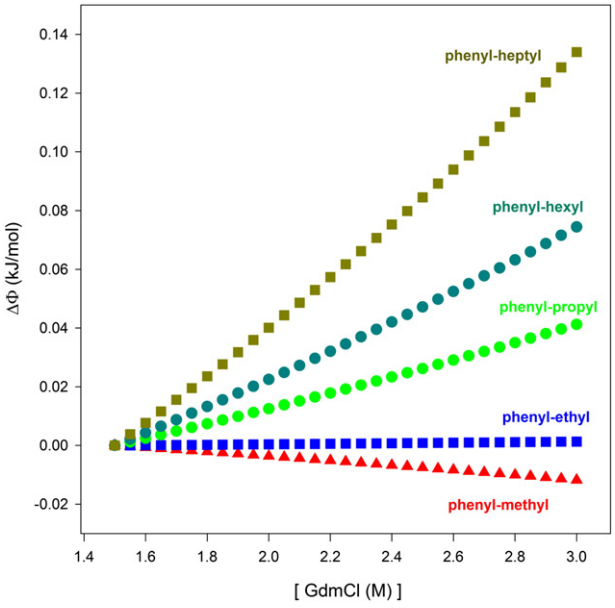

Fig. 4. GdmCl concentration dependence of ΔΦ as defined by Eq. (10). The initial slopes are: phenyl-methyl = −6.84E−03, phenyl-ethyl = 7.74E−04, phenyl-propyl = 2.36E−02, phenyl-hexyl = 4.23E−02, and phenyl-heptyl = 7.51E−02; the initial slopes have units of $\frac{kJ \cdot L}{mol^2}$.

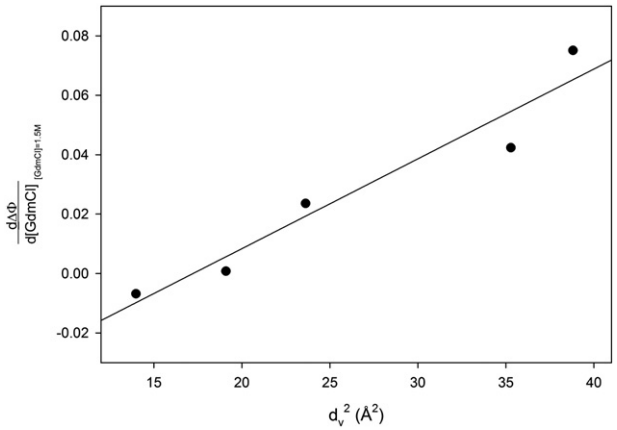

Fig. 5. Initial slope $\left[\frac{d(\Delta\Phi)}{d[\mathrm{GdmCl}]}\right]_{[\mathrm{GdmCl}]=1.5\ \mathrm{M}}$ values plotted as a function of hard sphere diameters of the alkyl tail groups, the diameters are obtained from Reference [32], the coefficient of determination of this plot is $r^2 = 0.93$.

$\left[\frac{d(\Delta\Phi)}{d[\mathrm{GdmCl}]}\right]_{[\mathrm{GdmCl}]=1.5\ \mathrm{M}}$ is plotted as a function of $(d_v)^2$ the cube of the hard sphere diameter [33] of the alkyl group, demonstrating a linear correlation with size.

This observed size dependence can be further explained if we adopt the formalism suggested by Graziano [34], in this case, $\Delta G_{\mathrm{alkyl}}$ can be broken up into two terms:

$$\Delta G_{\mathrm{alkyl}} = \Delta G_{cav} + \Delta G_{att} \tag{13}$$

where ΔG_{cav} represents the contribution from the reversible work that is required to make a cavity that will accommodate the alkyl group in the solvent and ΔG_{att} is the contribution from the reversible work that is required to turn on attractive interactions between the solvent molecules and the alkyl moiety, if we expand the derivative we obtain:

$$\frac{d(\Delta\Phi)}{d[\mathrm{GdmCl}]} = \frac{d(\Delta G_{cav})}{d[\mathrm{GdmCl}]} + \frac{d(\Delta G_{att})}{d[\mathrm{GdmCl}]} + (m - n + \alpha - \beta)\,. \tag{14}$$

The calculations of Graziano show that [35–37]: a) the addition of GdmCl makes it more difficult to form a cavity in the aqueous solution, this promotes hydrophobic contact-pair promotion; b) on the other hand, the addition of GdmCl increases the magnitude of attractive interactions between the alkyl moiety and the solvent molecules disrupting the hydrophobic contact pair. In other words, adding GdmCl makes ΔG_{cav} more negative while simultaneously making ΔG_{att} more positive. For spherical hydrophobic solutes both ΔG_{cav} and ΔG_{att} depend on the hydrophobic surface area, but the attractive interactions show a much sharper dependence on the cube of the solute diameter. Therefore, beyond a certain solute size, the attractive contributions will dominate the value of $\left[\frac{d(\Delta\Phi)}{d[\mathrm{GdmCl}]}\right]_{[\mathrm{GdmCl}]=1.5\ \mathrm{M}}$ resulting in the observed sign change. Based on these results we can suggest that guanidinium ions affect hydrophobic interactions in a size dependent fashion. The denaturant is either indifferent towards, or slightly stabilizes, the interactions between small hydrophobes; however, as the size of the interacting hydrophobes increases, the denaturant becomes more and more effective in disturbing the stability of contact pairs formed between the molecules.

4. Conclusions

In this work we have determined the effect of GdmCl on hydrophobic interactions between contact-pairs formed between phenyl and alkyl moieties. Due to the simplicity of our model system, we were able to isolate the effect of GdmCl on hydrophobic interactions. We were able to quantitatively show that the presence of GdmCl may stabilize smaller hydrophobic pairs; while, on the other hand, GdmCl was shown to destabilize hydrophobic contact pairs formed between phenol and larger hydrophobes. Our findings are in agreement with molecular dynamic simulations mentioned earlier [20], which showed that methane pairs are stabilized by the addition of GdmCl, but large hydrophobes are destabilized. These results are consistent with other observed experimental results. Guanidinium destabilizes micelles and lipid bilayers [38,39], which are considered to be large hydrophobes. Protein folding studies have also shown that interactions between small hydrophobes are being stabilized by GdmCl, causing residual order to persist in guanidinium unfolded protein, defining a non-random-coil denatured state [40–43].

The mechanism by which guanidinium chloride denatures proteins has been questioned and studied for many years. Folded proteins are extremely complex and there are numerous interactions that hold the protein's secondary and tertiary structure together. As an example, the main interactions are those of hydrogen bonding, electrostatic, and the hydrophobic effect. How these interactions are affected by the presence GdmCl is the main topic for discussion and it is still not clear which mechanism the denaturant partakes in to destabilize the folded structures of proteins. However, as far as simple hydrophobic interactions are concerned, the linear dependence of $\left[\frac{d(\Delta\Phi)}{d[\mathrm{GdmCl}]}\right]_{[\mathrm{GdmCl}]=1.5\ \mathrm{M}}$ on $(d_v)^2$ indicates that guanidinium interacts with hydrophobic molecules through surface-mediated interactions. This can be done through: *modulating hydrophobic hydration*, guanidinium is able to accumulate at the surface of hydrophobic molecules because it is first, weakly hydrated and breaks fewer hydrogen bonds while it accesses the hydrophobic surfaces [20,44,45] and second, the ion's planar shape allows it to stack parallel to the alkyl surface [20,44,45]; the stacking of the guanidinium ion also promotes a disruption of hydrophobic interactions between protein side chains through *van der Waals interactions between the denaturant and hydrophobic molecules* [20]. Hydrophobic dehydration and van der Waals interactions are surface-dependent, therefore, van der Waals interactions become more dominant when the denaturant is interacting with hydrophobes having large surfaces. This confirms that non-hydrogen bonding interactions play a role in the denaturating properties of the guanidinium ion. This being said, recent spectroscopic data [46,47] demonstrate that the addition of guanidinium ion changes the hydrogen bonding properties of the aqueous solvent system. Therefore, it is possible that a "unified description" similar to that suggested by Moeser and Horinek for urea, may provide a realistic picture of guanidinium denaturation [48].

Acknowledgments

This work was supported in part by the Natural Sciences and Engineering Research Council of Canada (NSERC) (314021-2012) and by the Graduate Enhancement of Tri-Council Stipends (GETS) program of the University of Manitoba.

References

[1] K.C. Aune, C. Tanford, Thermodynamics of the denaturation of lysozyme by guanidine hydrochloride. II. Dependence on denaturant concentration at 25 °C, Biochemistry 8 (1969) 4586–4590.
[2] B.J. Bennion, V. Daggett, The molecular basis for the chemical denaturation of proteins by urea, Proc. Natl. Acad. Sci. U. S. A. 100 (2003) 5142–5147.
[3] A. Caballero-Herrera, K. Nordstrand, K.D. Berndt, L. Nilsson, Effect of urea on peptide conformation in water: molecular dynamics and experimental characterization, Biophys. J. 89 (2005) 842–857.
[4] C. Camilloni, A. Guerini Rocco, I. Eberini, E. Gianazza, R.A. Broglia, G. Tiana, Urea and guanidinium chloride denature protein L in different ways in molecular dynamics simulations, Biophys. J. 94 (2008) 4654–4661.
[5] J.L. England, V.S. Pande, G. Haran, Chemical denaturants inhibit the onset of dewetting, J. Am. Chem. Soc. 130 (2008) 11854–11855.
[6] J. Heyda, M. Kozisek, L. Bednarova, G. Thompson, J. Konvalinka, J. Vondrasek, P. Jungwirth, Urea and guanidinium induced denaturation of a Trp-cage miniprotein, J. Phys. Chem. B 115 (2011) 8910–8924.

[7] A. Huerta-Viga, S. Woutersen, Protein denaturation with guanidinium: a 2D-IR study, J. Phys. Chem. Lett. 4 (2013) 3397–3401.
[8] T. Koishi, K. Yasuoka, S.Y. Willow, S. Fujikawa, X.C. Zeng, Molecular insight into different denaturing efficiency of urea, guanidinium, and methanol: a comparative simulation study, J. Chem. Theory Comput. 9 (2013) 2540–2551.
[9] F. Mehrnejad, M. Khadem-Maaref, M. Ghahremanpour, F. Doustdar, Mechanisms of amphipathic helical peptide denaturation by guanidinium chloride and urea: a molecular dynamics simulation study, J. Comput. Aided Mol. Des. 24 (2010) 829–841.
[10] J.K. Myers, C. Nick Pace, J. Martin Scholtz, Denaturant m values and heat capacity changes: relation to changes in accessible surface areas of protein unfolding, Protein Sci. 4 (1995) 2138–2148.
[11] C. Oostenbrink, W.F. van Gunsteren, Methane clustering in explicit water: effect of urea on hydrophobic interactions, Phys. Chem. Chem. Phys. 7 (2005) 53–58.
[12] D. Trzesniak, N.F.A. van der Vegt, W.F. van Gunsteren, Computer simulation studies on the solvation of aliphatic hydrocarbons in 6.9 M aqueous urea solution, Phys. Chem. Chem. Phys. 6 (2004) 697–702.
[13] D.B. Watlaufer, S.K. Malik, L. Stoller, R.L. Coffin, Nonpolar group participation in the denaturation of proteins by urea and guanidinium salts. Model compound studies, J. Am. Chem. Soc. 86 (1964) 508–514.
[14] Z. Xia, P. Das, E.I. Shakhnovich, R. Zhou, Collapse of unfolded proteins in a mixture of denaturants, J. Am. Chem. Soc. 134 (2012) 18266–18274.
[15] D.L. Beauchamp, M. Khajehpour, The effect of lithium ions on the hydrophobic effect: does lithium affect hydrophobicity differently than other ions? Biophys. Chem. 163–164 (2012) 35–43.
[16] D.K. Kunimitsu, A.Y. Woody, E.R. Stimson, H.A. Scheraga, Thermodynamic data from fluorescence spectra. II. Hydrophobic bond formation in binary complexes, J. Phys. Chem. 72 (1968) 856–866.
[17] R.D. Macdonald, M. Khajehpour, Effects of the osmolyte TMAO (trimethylamine-N-oxide) on aqueous hydrophobic contact-pair interactions, Biophys. Chem. 184 (2013) 101–107.
[18] A.Y. Moon, D.C. Poland, H.A. Scheraga, Thermodynamic data from fluorescence spectra. I. The system phenol-acetate, J. Phys. Chem. 69 (1965) 2960–2966.
[19] T.A. Shpiruk, M. Khajehpour, The effect of urea on aqueous hydrophobic contact-pair interactions, Phys. Chem. Chem. Phys. 15 (2013) 213–222.
[20] R. Godawat, S.N. Jamadagni, S. Garde, Unfolding of hydrophobic polymers in guanidinium chloride solutions, J. Phys. Chem. B 114 (2010) 2246–2254.
[21] P.E. Mason, J.W. Brady, G.W. Neilson, C.E. Dempsey, The interaction of guanidinium ions with a model peptide, Biophys. J. 93 (2007) L04–L06.
[22] E.P. O'Brien, R.I. Dima, B. Brooks, D. Thirumalai, Interactions between hydrophobic and ionic solutes in aqueous guanidinium chloride and urea solutions: lessons for protein denaturation mechanism, J. Am. Chem. Soc. 129 (2007) 7346–7353.
[23] W. Li, Y. Mu, Dissociation of hydrophobic and charged nano particles in aqueous guanidinium chloride and urea solutions: a molecular dynamics study, Nanoscale 4 (2012) 1154–1159.
[24] W.K. Lim, J. Rosgen, S.W. Englander, Urea, but not guanidinium, destabilizes proteins by forming hydrogen bonds to the peptide group, Proc. Natl. Acad. Sci. U. S. A. 106 (2009) 2595–2600.
[25] P.E. Mason, G.W. Neilson, C.E. Dempsey, A.C. Barnes, J.M. Cruickshank, The hydration structure of guanidinium and thiocyanate ions: implications for protein stability in aqueous solution, Proc. Natl. Acad. Sci. U. S. A. 100 (2003) 4557–4561.
[26] G.I. Makhatadze, P.L. Privalov, Protein interactions with urea and guanidinium chloride: a calorimetric study, J. Mol. Biol. 226 (1992) 491–505.
[27] D.R. Robinson, W.P. Jencks, The effect of compounds of the urea–guanidinium class on the activity coefficient of acetyltetraglycine ethyl ester and related compounds, J. Am. Chem. Soc. 87 (1965) 2462–2470.
[28] C.H. Chan, J.C. Escalante-Semerena, ArsAB, a novel enzyme from *Sporomusa ovata* activates phenolic bases for adenosylcobamide biosynthesis, Mol. Microbiol. 81 (2011) 952–967.
[29] J.R. Lakowicz, Principles of fluorescence spectroscopy, 3rd edition, Anal. Bioanal. Chem. 390 (2008) 1223–1224.
[30] B.J. Siwick, M.J. Cox, H.J. Bakker, Long-range proton transfer in aqueous acid-base reactions, J. Phys. Chem. B 112 (2007) 378–389.
[31] M. Namazian, S. Halvani, Calculations of pKa values of carboxylic acids in aqueous solution using density functional theory, J. Chem. Thermodyn. 38 (2006) 1495–1502.
[32] N.C. Price, R.A. Dwek, R.G. Ratcliffe, M.R. Wormald, Principles and Problems in Physical Chemistry for Biochemists, 3rd ed. Oxford University Press, Oxford, 2001.
[33] V. Gogonea, C. Baleanu-Gogonea, E. Osawa, Solvent hard sphere diameter from van der Waals volume A statistical analysis of computed and solubility determined solvent diameters, J. Mol. Struct. THEOCHEM 432 (1998) 177–189.
[34] G. Graziano, Role of salts on the strength of pairwise hydrophobic interaction, Chem. Phys. Lett. 483 (2009) 67–71.
[35] G. Graziano, On the size dependence of hydrophobic hydration, J. Chem. Soc. Faraday Trans. 94 (1998) 3345–3352.
[36] G. Graziano, On the solubility of aliphatic hydrocarbons in 7M aqueous urea, J. Phys. Chem. B 105 (2001) 2632–2637.
[37] G. Graziano, Contrasting the denaturing effect of guanidinium chloride with the stabilizing effect of guanidinium sulfate, Phys. Chem. Chem. Phys. 13 (2011) 12008–12014.
[38] J.K. Mahendra, Possible modes of interaction of small molecules with lipid bilayer in biomembrane, Proc. Indian Natl. Sci. Acad. 45 (1979) 567–577.
[39] R.J. Midura, M. Yanagishita, Chaotropic solvents increase the critical micellar concentrations of detergents, Anal. Biochem. 228 (1995) 318–322.
[40] P. Mandal, A.R. Molla, D.K. Mandal, Denaturation of bovine spleen galectin-1 in guanidine hydrochloride and fluoroalcohols: structural characterization and implications for protein folding, J. Biochem. 154 (2013) 531–540.
[41] R. Meloni, C. Camilloni, G. Tiana, Sampling the denatured state of polypeptides in water, urea, and guanidine chloride to strict equilibrium conditions with the help of massively parallel computers, J. Chem. Theory Comput. 10 (2014) 846–854.
[42] D.J. Segel, A.L. Fink, K.O. Hodgson, S. Doniach, Protein denaturation: a small-angle x-ray scattering study of the ensemble of unfolded states of cytochrome c, Biochemistry 37 (1998) 12443–12451.
[43] O. Zhang, J.D. Forman-Kay, Structural characterization of folded and unfolded states of an SH3 domain in equilibrium in aqueous buffer, Biochemistry 34 (1995) 6784–6794.
[44] Q. Shao, Y. Fan, L. Yang, Y.Q. Gao, Counterion effects on the denaturing activity of guanidinium cation to protein, J. Chem. Theory Comput. 8 (2012) 4364–4373.
[45] E. Wernersson, J. Heyda, M. Vazdar, M. Lund, P.E. Mason, P. Jungwirth, Orientational dependence of the affinity of guanidinium ions to the water surface, J. Phys. Chem. B 115 (2011) 12521–12526.
[46] J.N. Scott, N.V. Nucci, J.M. Vanderkooi, Changes in water structure induced by the guanidinium cation and implications for protein denaturation, J. Phys. Chem. A 112 (2008) 10939–10948.
[47] I.M. Pazos, F. Gai, Solute's perspective on how trimethylamine oxide, urea, and guanidine hydrochloride affect water's hydrogen bonding ability, J. Phys. Chem. B 116 (2012) 12473–12478.
[48] B. Moeser, D. Horinek, Unified description of urea denaturation: backbone and side chains contribute equally in the transfer model, J. Phys. Chem. B 118 (2014) 107–114.